DELTA UNIVERSITY
SCIENTIFIC JOURNAL
Journal home page: www.deltauniv.edu.eg/dusj

SUPERHYDROPHOBIC COPPER ALLOY SURFACE BY ELECTROPHORETIC DEPOSITION WITH CORROSION RESISTANCE AND IMPROVED ADHESION

Asmaa A. El-halag[1], Rafik Abbas[2],Aya A. Rahal[2], Wagih A. Sadik[2], Abdel Ghaffar M. El Demerdash[2]

[1]Assistant lecturer of Basic Science Department, Faculty of Engineering, Delta University for Science and Technology. Mansoura: Gamasa – Costal International Road in front of Industrial Area.

Research Assistant, Materials Science Department, Institute of Graduate Studies and Research, Alexandria University.

[2]Materials Science Department, Institute of Graduate Studies and Research, Alexandria University, Alexandria, Egypt.

Abstract

The superhydrophobicity is defined as a surface with both a water contact angle (CA) exceed 150° and a water sliding angle (SA) less than 10.0 , this strategy is clearly exhibited by the lotus leaf whose surface is structured on two length scales by micron and nano sized wax protrusions. Copper and its alloys have been one of the important materials in industry owing to its high electrical and thermal conductivities, mechanical workability and its relatively noble properties. It is widely used in many applications in electronic industries and communications as a conductor in electrical power lines, pipelines for domestic and industrial water utilities including seawater, heat conductors and heat exchangers. One of the major problems which face Cu is the corrosion, which leads resulting in lower device performance and failure.

In this work, stable superhydrophobic surfaces have been successfully fabricated on the copper substrates by electrodeposition process in an electrolytic solution containing myristic acid (MYA), different metal chloride salts, and ethanol without any post processing procedures. Two unique phenomena were achieved; the first phenomenon was a concurrent electrodeposition of the superhydrophobic coatings on both cathodic and anodic copper alloy surfaces. The second phenomenon was the development of an excellent adhesion of the superhydrophobic coatings. Scanning electron microscopy (SEM), Fourier-transform infrared (FTIR) spectrometer, Energy dispersive X-ray (EDX) and contact angle measurements have been performed to characterize the surface morphology, chemical composition and the superhydrophobic

property. In the presence of copper chloride, micro/nano scales flower-like structures were composed with maximum (CA>155°) and (SA<4°). The corrosion resistance of the prepared superhydrophobic coatings was measured by electrochemical impedance spectroscopy (EIS) and Tafel polarization measurements. The developed metal myristate superhydrophobic surface has excellent corrosion resistance with significant decrease in corrosion currents densities (i_{corr}), corrosion rates and double layer capacitance (C_{dl}), with simultaneous increase in polarization resistance (R_{ct}) values in 3.5 wt. % NaCl solutions. Furthermore, this method is rapid, cost effective and it will have great prospects for industrial applications.

Keywords*: Superhydrophobicity; Copper alloy; Electrodeposition; Myristic acid; Metal salts; Corrosion resistance; Adhesion.*

1. Introduction

Superhydrophobicity is a property of a coating or material with high water contact angle (CA) exceeds 150° and sliding angle (SA)/contact angle hysteresis less than 10°, this phenomenon is believed to be governed by a surface chemistry and a surface geometrical microstructure. Therefore, the combination of low surface energy materials and high surface roughness are the main requirements by which the surface wettability can be dramatically enhanced. In nature, certain plant leaves, such as Lotus leaves, are known to be superhydrophobic and self-cleaning due to the hierarchical roughness of their leaf surface [1]. A similar effect, pond skaters (Gerris remigis) have the ability to stand and walk upon a water surface without getting wet [2]. Wettability of solid surfaces is an important phenomenon in our daily life, especially for superhydrophobic surfaces that have attracted great attention because of their interesting properties and important applications including separation of oil/water dispersions, self-cleaning, drag reduction, anti-fogging, anti-bacteria, anti-fouling, anti-icing, corrosion resistance, antireflection and stain-resistant surfaces [3]. In the last decade, several techniques have been developed to fabricate artificial superhydrophobic surfaces, including plasma etching [4], sol-gel method [5,6], layer-by-layer deposition [7,8], spraying [9,10], chemical vapor deposition [11], electrospinning [12], hydrothermal process[13], electrochemical deposition,[14-21]. Electrodeposition has emerged as a competitive technique for the advantages over other techniques because of easy control of the thickness of the surface; simplicity; inexpensive equipment, and the possibility of making large surface area. However, there is a limited published literature concerning a rapid one-step process to simultaneous fabrication of two anodic and cathodic superhydrophobic coatings [17]. Such system presents a rapid electrodeposition method for constructing environmentally stable superhydrophobic coatings on cathodic and anodic surfaces, respectively. On the other hand, Copper and its alloy are widely used in different applications, and its corrosion imposes a major

challenge. Application of electrodeposition process on copper will present a solution to the long-standing problems of environmental contamination and corrosion of the metal and its alloys [22].

Many researches are developing to fabricate superhydrophobic cathodic surface by electrodepositing on copper plate. The aim of this work is to considered extension to the previous studies by using new and different metal salts. The initial purpose of this study is to prepare some effective structures on copper alloy surfaces using electrodeposition method which exhibit high superhydrophobic properties without introducing surface modifiers or other post-treatment procedures. The electrolyte solution will be made of myristic acid (MYA), different chlorides such as metal salts ($CuCl_2$, $FeCl_3$or $ZnCl_2$) and ethanol. The effect of different electrodeposition process parameters (deposition time, type and concentration of metal salt, concentration of myristic acid) on the surface morphology and wettability will be investigated. The anti-corrosion property of the developed superhydrophobic copper surface will be studied by electrochemical techniques. Besides, adhesion of the prepared coatings on the substrate will be also evaluated as well.

2. Experimental

2.1. Materials

Ethanol (95 %), was purchased from Elnasr pharmaceutical Chemical Company, Alexandria, Egypt) and used as received. Copper chloride dihydrate ($CuCl_2.2H_2O$), Zinc chloride ($ZnCl_2$), Ferric chloridehexahydrate ($FeCl_3.6H_2O$) and Myristic acid (MYA, $C_{14}H_{28}O_2$) were purchased from (Alpha Chemika, India).Silicon carbide sandpaper (from 400 to 800 grades) were obtained from Emery cloth sandpaper factory, China.

2.2. Sample Preparation

All prepared surface were produced using the same procedure. The detailed process was as follows; First, two cleaned copper alloy specimens with dimensions of 60 mm×25 mm×0.3 mm were abraded using silicon carbide papers (from 400 to 800 grades), washed with a distilled water and ethanol followed by drying in air. Second, different metal salts ($CuCl_2$, $FeCl_3$ or $ZnCl_2$) with specific amounts were added to certain mass of myristic acid and dispersed in ethanol under stirring until a uniform electrolyte solution (50 ml) was obtained. Third, the two prepared copper alloy specimens were taken as the cathode and anode in the electrolytic cell. DC voltage of 30 V was applied to the electrodes with a separating distance of 2 cm, where the copper electrode had a current density value of 0.0059 A/cm^2. Finally, after a certain electrolysis time, the working electrodes were rinsed thoroughly several times in distilled water, and then air dried. Subsequently, superhydrophobic surface with micro/nano structures on the cathodic and anodic plates were obtained.

2.3. Sample Characterization

The surface morphology of the developed cathodic and anodic

superhydrophobic copper alloy substrates were characterized by scanning electron microscopy (SEM, JSM-6390A).An energy dispersive X-ray spectrum (EDX) was also used to analyze the micro zone elemental composition of the surface. The Fourier-transform infrared (FTIR) were recorded at room temperature on Fourier-transform infrared spectrophotometer (FTIR, Bruker-Tensor27). Different spectra were collected over the range of 500–4,400 cm^{-1}.The surface wettability was evaluated by contact angle (CA) measurements using Gaosuo USB digital microscope (magnification range 1 X ~ 500 X), all the angles were determined by averaging values measured at five points on different locations on each sample surface. Besides, the adhesion of the superhydrophobic coatings on copper substrate were carried out according to the ISO-2409 standard tape test method using Cross Hatch Cutter, model Elcometer 107.

2.4. Electrochemical Measurements

The corrosion resistance of the samples was investigated via potentiodynamic polarization curves and electrochemical impedance spectroscopy (EIS) acquired by electrochemical experiments in 3.5 wt. % NaCl solution. Electrochemical experiments were performed using a computer-controlled electrochemical system (GAMRY PCI4G750 instruments) at room temperature, equipped with a standard three-electrode system with an Ag/AgCl reference electrode, a platinum (Pt) wire as the counter electrode (CE), and the sample with an exposed area of 1.0 cm^2 as the working electrode (WE). Prior to potentiodynamic polarization and electrochemical impedance spectroscopy measurements, 1 h immersion was given to ensure the steady state. EIS was performed in the frequency range between 10 MHz and 100 kHz. Polarization curves (Tafel plots) were acquired at a scanning rate of 1mV/s from -0.25 to 0.25 V. The corrosion current density (i_{corr}) for the specimens was determined by extrapolating the anodic and cathodic Tafel slopes. All EIS spectra were analyzed in Nyquist representation.

3. RESULTS AND DISCUSSION

3.1. Surface Morphology

Two superhydrophobic coatings were simultaneously fabricated on cathodic and anodic copper surfaces from an electrolyte solution including copper chloride, myristic acid, and ethanol. The morphology evolution of the prepared cathodic and anodic copper surface using copper chloride salt (0.025M) and (0.1 M) myristic acid for various electrolysis times is shown by the SEM as shown in figure (1).

The morphology for the cathodic surface with deposition time of 10 min shows very small flower-like structures in micro-nano arrangements after electrodeposition process, with a contact angle of 157.8 ± 1.1°. It is reasonable to expect that the microstructure trap lots of airs, and the air layer can effectively prevent water from penetrating the surface and also it could be seen from the water drop shape, as shown in figure (1-a). With increasing the deposition

time to 15 min, the superhydrophobic coating becomes very thick and the flower-like structures merge to large-scale structures and the contact angle reduces to 150 ± 1.3^{o}(figure (1-b). This is mainly due to it is too large to suppose water drop and then superhydrophobicity is significantly weakened [21].

The surface morphology of the anodic copper alloy surfaces at different deposition times is shown in figure 1(c and d).It can be seen from figure 1c that small uniform needles appear on the anodic surface after 10 min deposition time, and it has a contact angle of 152.9 ± 0.9^{o}.However, when deposition time prolongs to 15 min, the needles number increase with slight increase in the CA value of 153.5 ± 0.8^{o}, as shown in figure. 1d. Therefore, deposition times 10 and 15 min, for anodic deposition create nearly the same surface morphology, as shown from their relevant CAs values.

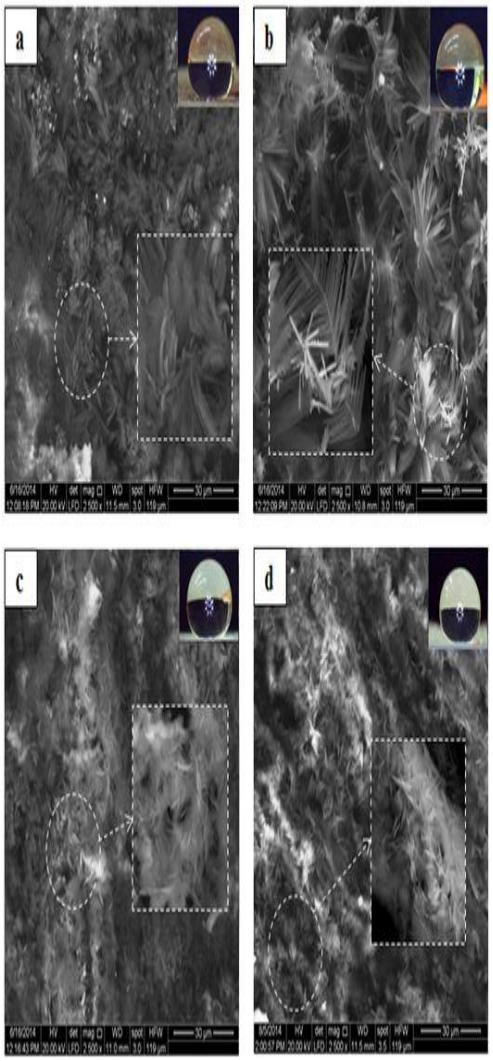

Fig. 1. SEM images of copper alloy surfaces at 0.025 M copper chloride with 0.1 M myristic acid solution; cathodic deposition for (a) 10 min, (b) 15 min, anodic deposition for (c) 10 min and (d) 15 min.

In order to validate the method's applicability, other metal salts were used. Copper chloride salt was replaced by both ferric or zinc chloride salts which generate only cathodic superhydrophobic surfaces. Ferric chloride shows plentiful micro-nano structures of the cauliflower-like hierarchical that exhibit CA of 165 ± 0.3^{o}, whereas the surface morphology of

zinc chloride shows flaked shapes with CA of 159.2 ± 0.6º (figure 2).

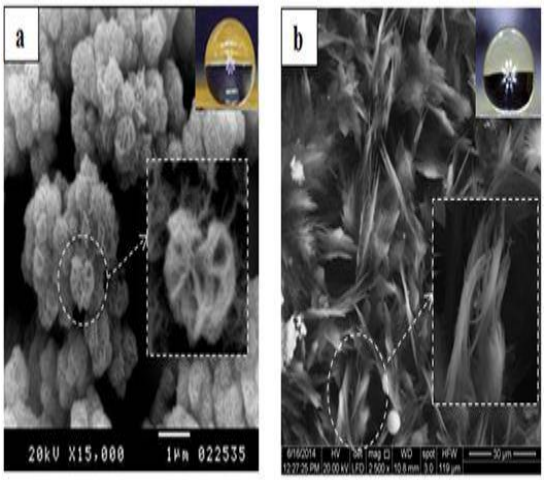

Fig. 2. SEM images of cathodic copper surface using different metal salts; (a) FeCl3 and (b) ZnCl2.

3.2. Chemical Characterization

In this work, FTIR and EDX were used to analyze the chemical composition of the prepared both cathodic and anodic superhydrophobic surfaces. Figure 3 shows the FTIR of the powders scraped from both superhydrophobic surfaces (anodic and cathodic) at 30 V DC for 10 min. In the low-frequency region, it is well known that the carboxyl group (COO) from myristic acid appears at 1698 cm^{-1}, as shown in spectrum 1. After the electrodeposition process, the absorption peak for free (COO) from myristic acid at 1698 cm^{-1} was absent. Whereas both cathodic and anodic superhydrophobic surfaces exhibited the adsorption peaks at 1624, 1465 cm^{-1} and at 1628, 1540 cm^{-1}, as shown in spectra 2 and 3 of figure 3, respectively. The absorption peaks may stem from asymmetric and symmetric stretches of coordinated (COO) moieties of cathodic and anodic superhydrophobic surfaces, respectively [23]. In the high-frequency region, the spectra of both superhydrophobic surfaces and pure myristic acid shows the absorption peaks at about 2920 cm^{-1} and 2851.3 cm^{-1} which is attributed to C–H asymmetric and symmetric stretching vibrations, respectively. In addition, the peak appears at 3494 cm^{-1} is due to the O–H group. Besides, the new peaks which appear in the finger print region of spectrum 3 at 905.92, 723.36 and 467.03 cm^{-1} of the anodic coatings are assigned to the formation of $Cu_2(OH)_3Cl$ [17, 24].

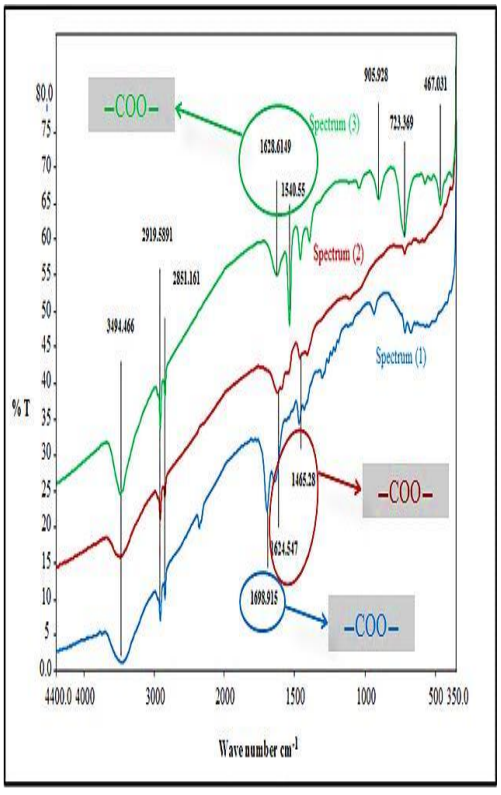

Fig. 3. FTIR spectrums of myristic acid (spectrum 1), powders scraped from the cathodic superhydrophobic surface (spectrum 2) and the anodic superhydrophobic surface (spectrum 3).

The elemental analysis of cathodic and anodic coatings was investigated by EDX technique (figure 4).The presence of C, O and Cu elements confirmed the formation of copper myristate (Cu [CH_3 $(CH_2)_{12}COO]_2$) on both cathodic and anodic surfaces, and the Cl peak probably results from remaining copper chloride. The amount of Cl element on the cathodic electrode is negligible compared to the anodic electrode which confirms the formation of $Cu_2(OH)_3Cl$ species on the anodic electrode only as proved from FTIR results. Consequently, based on EDX and FTIR analysis, it can be deduced that Cu myristate, with low surface energy, was formed on both superhydrophobic surfaces.

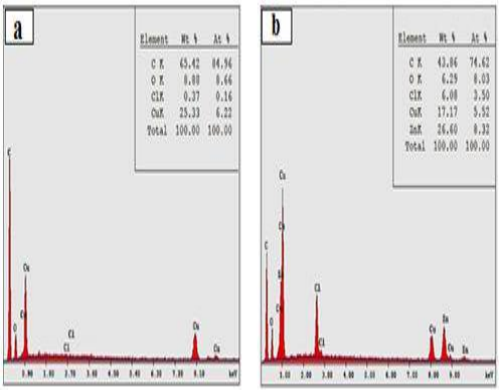

Fig. 4. EDX spectra of superhydrophobic copper alloy surfaces with copper chloride metal salt (a) cathodic and (b) anodic surfaces.

Furthermore, the obtained results were related to the formation mechanism of electrodeposition. The detailed explanation is shown in figure 5. When the copper electrodes were immersed in the electrolyte solution with the application of DC voltage, some Cu^{+2} ions near the cathode have been reacted with myristic acid, and Cu myristate and hydrogen ions are formed on cathodic surface. Meanwhile, free H^+ ions will also increase, and some H^+ ions can get electron and then forms H_2 [21,23]. Simultaneously, Cu^{+2} and Zn^{+2} ions which are related to the copper alloy ionization; immediately combine with residual myristate $[CH_3(CH_2)_{12}COO]^-$ to form $(Cu[CH_3(CH_2)_{12}COO]_2)$ and $(Zn[CH_3(CH_2)_{12}COO]_2)$ complexes. The copper myristate deposits on anodic copper alloy were higher than the solubility of electrolyte. Moreover, Cl^- ions in the electrolyte solution migrate to the anode and react with Cu^{2+} and OH^- to form copper trihydroxyl chloride $Cu_2(OH)_3Cl$ complex [17,20] that precipitates on the anodic plate. Equations (1-4) describe the cathodic reactions process and while equations (5-7) describe the anodic reactions process.

$$Cu2+ + 2e- \rightarrow Cu$$

$$Cu2+ + 2\,CH3(CH2)12COOH \rightarrow (Cu[CH\square(CH2)12COO]2) + 2H+$$

$$2H+ + 2e- \rightarrow H2$$

$$Cl- + H+ \rightarrow \square Cl$$

$$Cu2+ + 2\,CH3(CH2)12COOH \rightarrow (Cu[CH\square(CH2)12COO]2) + 2H+$$

$$Zn2+ + 2\,CH3(CH2)12COOH \rightarrow (Zn[CH\square(CH2)12COO]2) + 2H+$$

$$Cu2+ + 2Cl- + OH- \rightarrow C\square 2(OH)3Cl$$

Similar to the cathodic deposition of copper chloride, the cathodic products formed in case of ferric and zinc chloride salts were ferric myristate and zinc myristate, respectively.

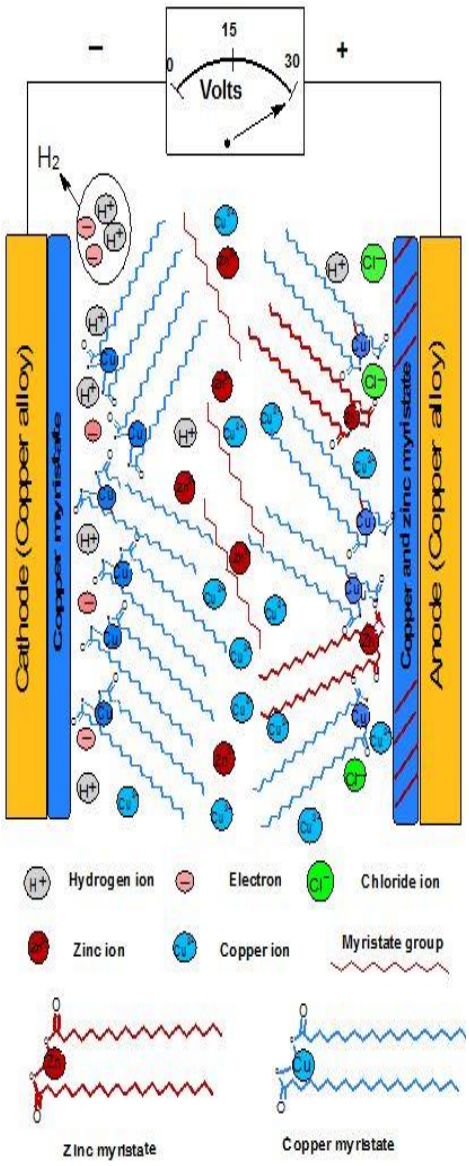

Fig. 5. The electrodeposition mechanism.

3.3. Surface Wettability

The surface wettability of the obtained surfaces on the copper substrate with different surface morphology has been studied by CA measurements. The surface wettability of the developed superhydrophobic copper alloy substrates was affected by the deposition time and the concentration of both fatty acid and metal salts. Figures 6 and 7 demonstrated the relationship between the contact angle of cathodic and anodic surfaces and the concentration of myristic acid at 0.025 M copper chloride for 3, 5, 10, 15 min, respectively. For cathodic surface, 0.1 M myristic acid shows the highest CA of 156.8 ± 1º. The prepared surface exhibits the micro- and nano- scale hierarchical structure, which has great porosity and surface roughness. Air could be trapped easily within the structure, so the CA value of the surface was very high. However, when the acid concentration increases up to 0.2 M, the effective structure was no longer found in the prepared surfaces with an obvious decrease in the CA value (134.5 ± 2.3º), (see Fig.6). The products do not show the micro- and nanoscale hierarchical structure, great porosity and surface roughness. Thus, the CA values of the products began to decline, until the highest (the acid concentration was 0.2 M). Therefore, water droplets could easily penetrate the superhydrophobic coating causing a decrease in CA and weakened the superhydrophobic property with unstable and non-homogenous coating layer.

Unlike cathodic deposition, the anodic deposition shows a different behavior; as with the increase in the concentration of myristic acid, the contact angle first increases and then decreases (figure 7). The increase and the decrease in contact angle can be attributed to the co-existence of the micro/nano rough morphology surface with increased number of needles, the increased needles intensity of copper myristate with low surface energy, and together reducing the affinity of water toward the

surface. Further increase in the amount of myristic acid, changes the micro-nano scale into millimeter scale which decreases the surface roughness and increase the inter-space distances which resulted in lower value of CA.

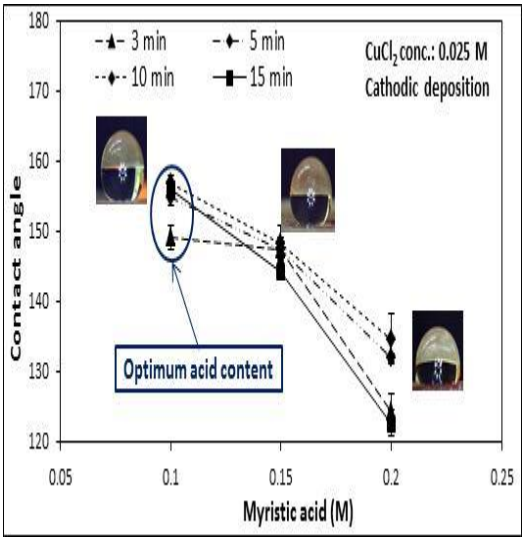

Fig. 6. The effect of myristic acid concentration at different deposition times on the wettability of cathodic surface.

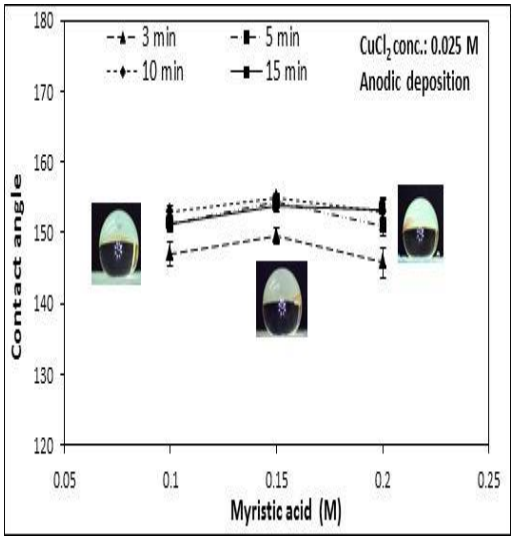

Fig. 7. The effect of myristic acid concentration at different deposition times on the wettability of anodic surface.

The effect of copper chloride salt concentration on the contact angle at different deposition times was studied (figures 8 and 9). For cathodic surface, the optimum copper chloride concentration was 0.025 M which shows the highest CA of 157.8 ± 0.9º at optimum deposition time of 10 min. Further increase in $CuCl_2$ concentration and deposition time shows a decrease in the CA value as the coatings become thicker and weakly-adhered to the surface, which weakens the effect of micro/nano scales structure on the superhydrophobic property (figure 8). As for anodic surface, the optimum copper chloride concentration was 0.04 M that shows the highest CA of 155 ± 1.5º at deposition time of 15 min. Lower deposition times shows smaller CAs as the anodic reaction needs more time to form a uniform superhydrophobic coating on the anodic surface**.**

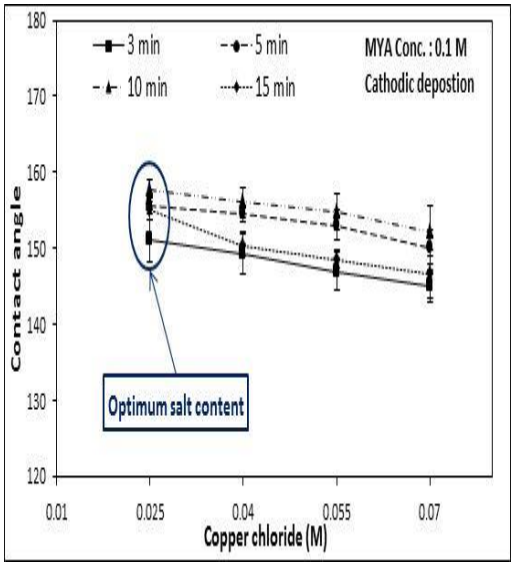

Fig. 8. The effect of copper chloride concentration at different deposition times on the wettability of cathodic surface.

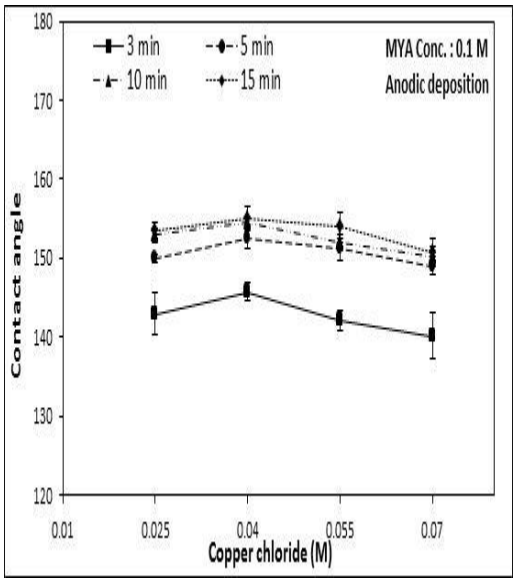

Fig. 9. The effect of copper chloride concentration at different deposition times on the wettability of anodic surface.

According to Cassie Model, air is trapped in groove of superhydrophobic film [25], and water contacts with superhydrophobic surface through an interface composed of both solid part and air. Apparent contact angle θr of coated Cu can be expressed as given by equation (8) [25].

$$\cos\theta r = f1\cos\theta - f2 \quad (8)$$

Where f_1 and f_2 are fractions of solid surface and air in contact with water, respectively, θr and θ are water contact angles on rough and smooth surfaces, respectively. Moreover, the molecular structure of myristic acid is composed of a long hydrocarbon chain which has low surface energy provides superhydrophobic property. The coated film obtained can be idealized as a rough surface with $-CH_3$ group exposed to air. According to previous reports [26] contact angle of water on flat surface is in the range of 113–115°. As can be seen from figure 4, the maximum contact angle on the superhydrophobic rough surface was 156.80. When these angles are introduced into equation (8), it was estimated that f_1 is 0.1397 and f_2 is 0.8603. The high values of f_2 suggest that superhydrophobic surfaces had more air among the micro/nano structures than the smooth surface, which is responsible for the superhydrophobic property.

The same results were obtained for cathodic electrodeposition using myristic acid with other metal salts ($FeCl_3$ and $ZnCl_2$). The optimum deposition time for zinc chloride and ferric chloride salts were 3 and 5 min with CAs of 159.2 ± 1.1° and 165 ± 0.4°, respectively. The optimum performance of different metal chloride salts on the surface wettability of copper alloy electrodes are summarized in figure 10.

Different stain droplets on the surface of the coated cathodic and anodic copper surfaces are shown in figure 11. All droplets show spherical shapes and easily rolled off from the superhydrophobic surface leaving the surface very clean and unaffected by stains.

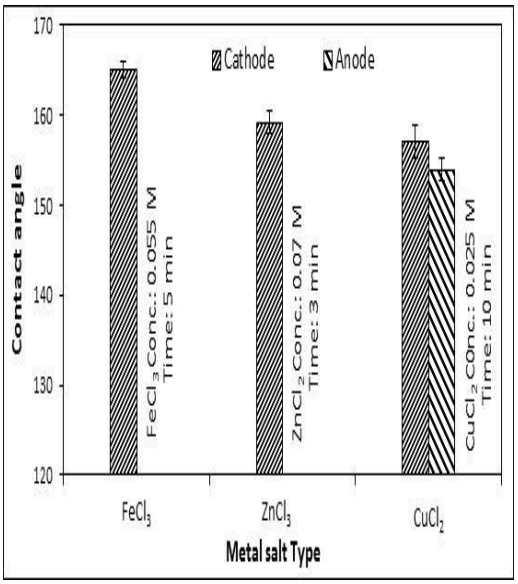

Fig. 10. The optimum performance of different metal chloride salts on the surface wettability of copper alloy surfaces.

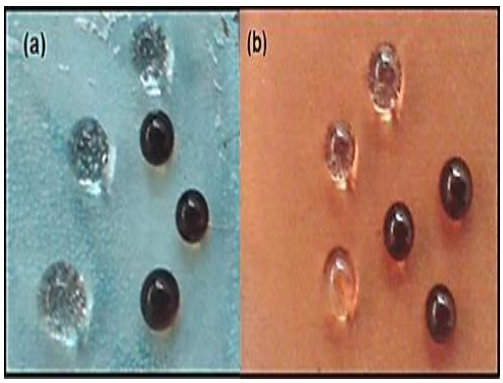

Fig. 11. Different stain droplets on the surface of superhydrophobic copper alloy electrodes (a) anodic layer and (b) cathodic layer.

3.4. Corrosion Resistance Performance

3.4.1. Electrochemical impedance spectroscopy (EIS)

In order to explore the corrosion resistance ability of the superhydrophobic films in 3.5 wt. % NaCl aqueous solution, the electrochemical technique of EIS was applied. Figure 12a shows the EIS results in the form of Nyquist plots, in which the imaginary impedance (Z_{im}) was plotted against the real impedance (Z_{re}). For comparison, we tested the EIS of the bare copper alloy substrate and the different coated copper substrates in 3.5 wt. % NaCl aqueous solution. It has seen that the EIS responses are featured with similar capacitance loop over the whole frequency range, but the impedance values are different from each other. The impedance spectra (figure 12a) of the coated sample immersed in 3.5 wt. % NaCl displayed a tremendous impedance semicircles diameter whose diameter value was around ten of $k\Omega.cm^2$. The coated surface possessed an excellent anticorrosion property, which indicating that the coated film was sufficiently densely packed to prevent the diffusion of oxygen to the copper substrate and thus inhibits corrosion of the copper alloy substrate. The same previous data was also displayed using Bode plot which shows the relation between the frequency (log f) with the equivalent impedance (log z) and phase angle (θ), as shown in figure 12 b and c, respectively.

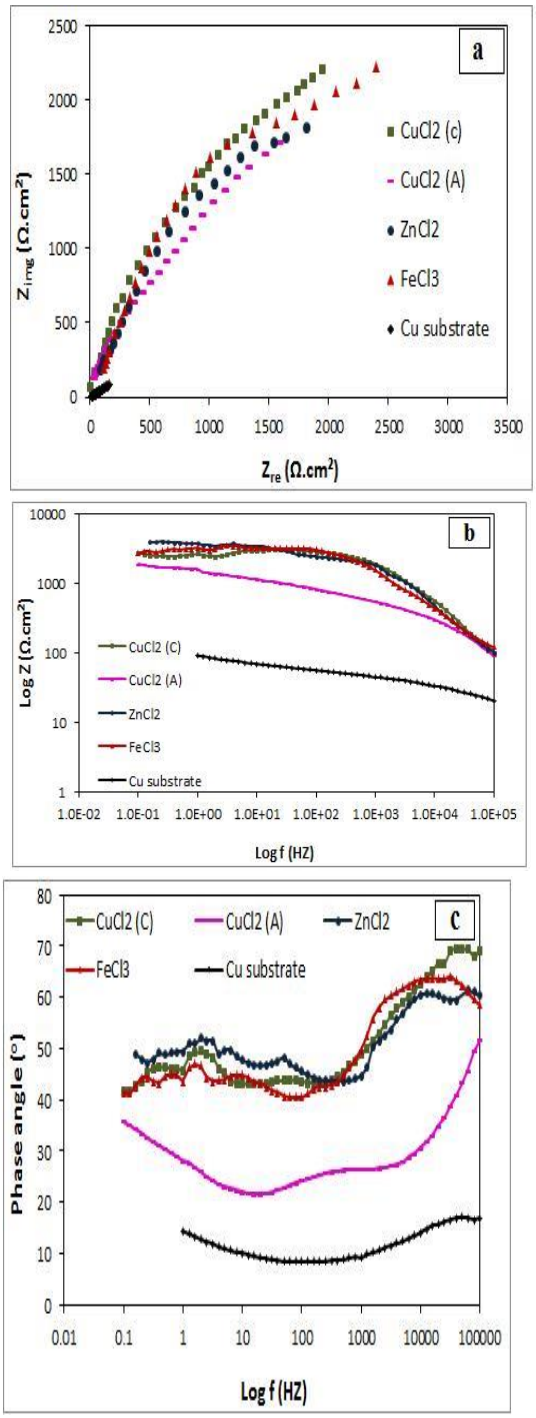

Fig. 12. (a) Nyquist diagrams for blank copper substrate and the superhydrophobic surfaces prepared with different metal salts in 3.5 wt. % NaCl solution, (b) and (c) Bode diagrams of measured EIS, (b) impedance magnitude; (c) phase angle.

The corresponding equivalent circuits for EIS test were proposed to further and quantitative analysis of corrosive behavior of the superhydrophobic surface and bare copper alloy substrate. The circuits as shown in figure 13a shows the equivalent circuit of the bare substrate, where R_u represents the solution resistance, C_{dl} is the capacitance of the electrical double layer, and R_{ct} is the charge transfer resistance. For superhydrophobic surface, the circuit as shown in figure 13b where R_{ct} // C_{dl} represent the impedance connected with the interface reactions and the solid state conduction in the barrier layer. C_c would normally be assigned to the capacitance of the intact coating (a function of factors such as film thickness and defect structure).Its value is much smaller than a typical double layer capacitance. The resistance R_{po} (pore resistance) could be attributed to the resistance of ion conducting paths that develop in the coating (governed mainly by pore dimensions). The resistance R_{po} of superhydrophobic specimen appeared considerably in comparison with the bare specimen (Table 1). It appears reasonably to conclude that the surface has been coated well and the pores are mostly sealed. The R_{ct} values in low frequency increase rapidly when the superhydrophobic film formed on the surface (shown in figure 12 and Table 1). It is proved that the superhydrophobicity plays an important role in improving the anticorrosion of the copper [27, 28].

The calculated equivalent circuit parameters for bare substrate and

superhydrophobic surface are presented in Table 1. Additionally, the areas covered with the superhydrophobic coatings are electrochemically inert and all the current is passed via pinholes on the electrode [28, 29]. The degree of the metal surface coverage (θ) is calculated from the following equation;

$$\theta = 1 - \frac{Rto}{Rt} \qquad (8)$$

Where R_{t_o} is charge transfer resistance of bare Cu, and R_t ($R_t = R_{ct} + R_{po}$) is the charge transfer resistance of the coated copper. The high percent coverage of coated copper surface shows decreasing in the defects of the surface. The coverage of superhydrophobic coatings is reached to 98%, showing excellent inhibition effect. In other words, both EIS plots and the electrochemical parameters calculated from EIS indicate that superhydrophobic surface can improve the corrosion resistance of copper alloy significantly.

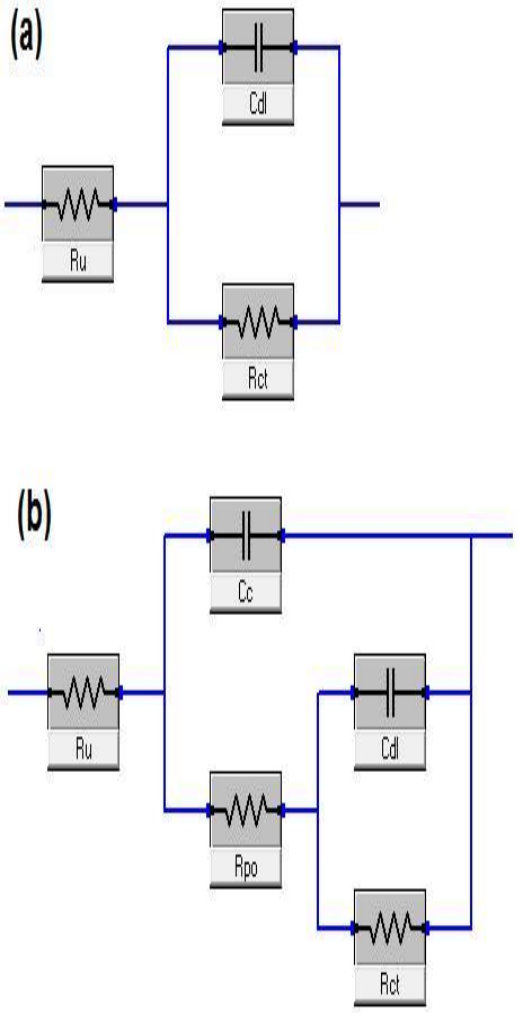

Fig. 13. Equivalent circuits used to fit the experimental data of EIS plots in Fig 7: (a) blank copper alloy substrate and (b) the superhydrophobic coated copper specimens.

Table 1. Electrochemical model impedance parameters derived from EIS.

Specimen	R_{ct} (kΩcm)	C_{dl} (μf)	n_1	R_{po} (kΩcm)	C_c (μf)	n_2	R_u (Ω)	% Coverage (θ)
Cu substrate	0.0911	124	0.656	-	-	-	2.5	-
Cathodic copper film	4.506	2.91	0.276	0.186	0.113	0.787	0.198	98.05
Anodic copper film	2.675	3.48	0.429	0.120	0.588	0.740	0.07	96.53
Cathodic ferric film	4.969	3.84	0.429	0.375	0.27	0.724	11.34	98.26
Cathodic zinc film	4.03	1.80	0.02	0.460	0.242	0.687	10.3	97.99

Table 1

3.4.2. Potentiodynamic polarization

Figure 14 shows Tafel polarization (E vs. log i) plots of the different superhydrophobic coatings electrodeposited on Cu surface in neutral 3.5 wt. % NaCl solution. The polarization curve for bare copper alloy substrate is also introduced for comparison. Corrosion potential (E_{corr}) and corrosion current density (i_{corr}) are often applied to evaluate the corrosion protective property of the coatings. The i_{corr} and E_{corr} are extracted from the intercept of Tafel slopes using Tafel extrapolation method are given in Table 2, also, the corrosion rate was presented. The inhibition efficiency (IE) is calculated using the following formula:

$$\mathbf{IE} = \frac{i - io}{i} \times \mathbf{1\square 0} \quad (9)$$

Where i and i_o mean the corrosion current densities of copper alloy electrodes covered with and without superhydrophobic coatings, respectively. The inhibition efficiency of the copper alloy with different superhydrophobic films surface is > 99.5 % (Table 2). The superhydrophobic surface has a better corrosion protection compared with the bare one. Theoretically, to increase corrosion resistance of a metal surface, it would be very effective to minimize the wetted area on a solid surface. As mentioned before, once the superhydrophobic coatings of Cu, Zn and Fe film on copper alloy surface immersed in the NaCl solution, the air could be trapped in the surface grooves which reduced the actual area of surface in contact with the solution. Therefore, the penetration of corrosive liquid or (Cl^-) ions will not reach the superhydrophobic copper alloy surface. This phenomenon supported the improvement of corrosion, therefore generated a better corrosion resistance.

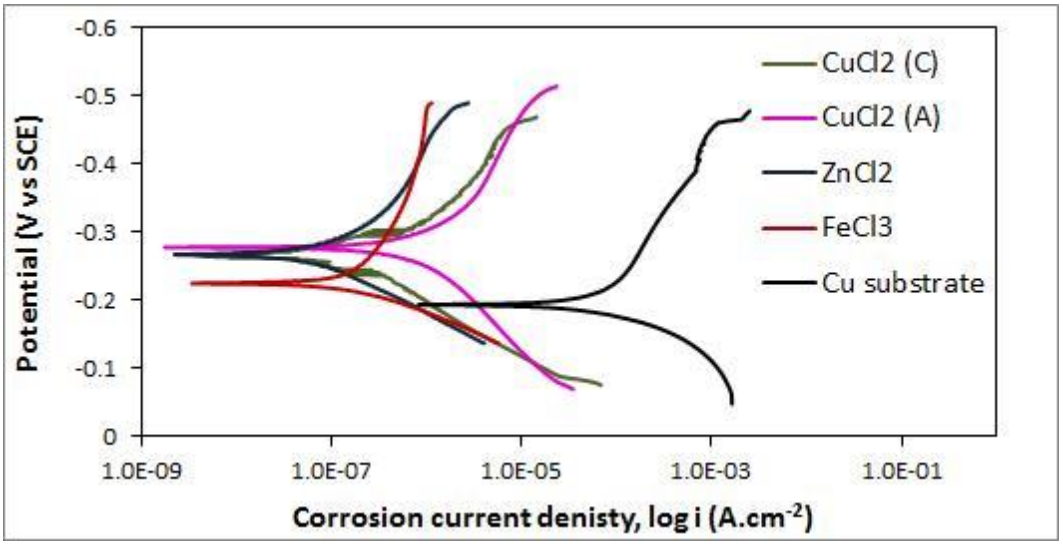

Fig. 14. Potentiodynamic polarization curves of blank copper substrate and the superhydrophobic surfaces prepared with different metal salts in 3.5 wt. % NaCl solution.

Table 2. Parameters extracted from polarization plots.

Specimen	i_{corr} ($\mu A\ cm^{-2}$)	E_{corr} (mV vs. Ag/AgCl)	Corrosion rate (m/y)	Efficiency (IE) %
Cu substrate	94.2	-206	63.79	—
Cathodic copper film	0.048	-266	0.089	99.95
Anodic copper film	0.198	-229	0.165	99.7
Cathodic ferric film	0.11	-235	0.109	99.88
Cathodic zinc film	0.139	-268	0.043	99.85

3.5. Adhesion Evaluation

The adhesion strength of the superhydrophobic coatings greatly influences the quality and life time of the developed superhydrophobic substrates. In this study, adhesion strength of different prepared superhydrophobic copper alloy surfaces was evaluated using the Tape Test (ISO-2409: Standard Test Methods for Measuring Adhesion by Tape Test) [30]. Figure 15 shows the optical images of the Fe superhydrophobic copper surface before and after the tape test. Figure. 15b clearly indicates that the superhydrophobic surface has a good adhesion property. The edges of the indented squares are completely smooth and did not detach after applying the tap. According to the ISO standard, the Fe coating is classified as Zero grade. Besides, all the droplets show spherical shape and the value of CA did not change after adhesion test. This indicates that the superhydrophobicity was not affect by test. Adhesion results of copper chloride salt for the cathodic layer showed adhesion performance with grade two

and for the anodic layer with grade three. Zinc chloride salt show very weak adhesion strength with grade five. Therefore, taking adhesion in consideration, ferric chloride salt will provide superior adhesion performance compared to the effect displayed by other metal salts.

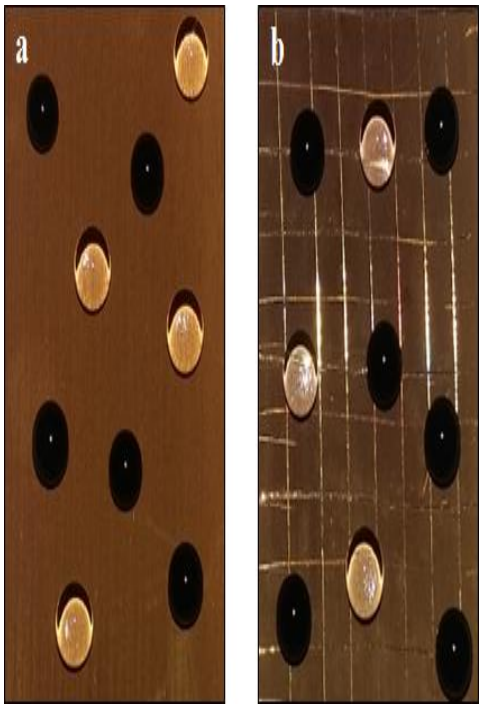

Fig. 15. Superhydrophobic copper alloy surfaces prepared with FeCl3 salt (a) before and (b) after the tape test.

4. Conclusions

A facile, fast and one-step electrodeposition process was applied to develop superhydrophobic surface on the copper alloy substrate with an electrolyte solution of myristic acid and different metal salts (namely; copper chloride, zinc chloride and ferric chloride) in ethanol solution. The hierarchical rough micro nanostructures of Cu/Zn myristate (Cu $(CH_3(CH_2)_{12}COO)_2$) with low surface energy is contributed an important role in the formation of superhydrophobicity. The effect of different parameters such as the concentration of fatty acid, metal salts and the deposition time on the properties of the prepared superhydrophobic surfaces was studied. The incorporation of copper chloride salts result in fabrication superhydrophobic coating on both cathodic and anodic copper electrodes simultaneously with CA >155° and SA < 4°, whereas zinc chloride and ferric chloride led to fabrication of only cathodic superhydrophobic coatings on copper alloy surfaces. All the prepared superhydrophobic coatings show excellent superhydrophobic properties and superior corrosion resistance when immersed in 3.5 wt.% NaCl solution due to the formation of air bags on the coating surface that prevent its attack with corrosive solutions. The analysis of potentiodynamic polarization, EIS and appropriate equivalent circuit models reveal that the copper alloy corrosion is effectively inhibited by the formation of a stable super-hydrophobic film. Adhesion measurements show that ferric chloride salt provided the best adhesion strength with grade zero which provides a new approach to expand the application of copper alloy in large-scale industrial applications.

References:

1- Liu, T, Chen, S, Cheng, S, Tian, J, Chang, X, Yin, Y, "Corrosion behavior of superhydrophobic surface on copper in seawater. "Electrochim. Acta, 52 (28) 8003–8007 (2007).

2- Bhushan, B, Jung, YC, "Natural and biomimetic artificial surfaces for superhydrophobicity, self-cleaning, low adhesion, and drag reduction."Prog.Mater.Sci.,56 (1) 1–108 (2011).

3- Valipour, NM, Birjandi, FC, Sargolzaei, J, "Super-non-wettable surfaces : A review. "Colloids Surf.A, 448 93–106 (2014).

4- Yan, YY, Gao, N, Barthlott, W, "Mimicking natural superhydrophobic surfaces and grasping the wetting process : A review on recent progress in preparing superhydrophobic surfaces."Adv. Colloid.Interface Sci.,169 (2) 80–105 (2011).

5- Latthe,SS,Imai,H, Ganesan,V, Rao,AV, "Superhydrophobic silica films by sol–gel co-precursor method."Appl. Surf. Sci.,256 (1) 217–222 (2009).

6- Xiu,Y, Hess,DW, Wong,CP ,"UV and thermally stable superhydrophobic coatings from sol – gel processing."J. Colloid Interface Sci.,326 (2) 465–470 (2008).

7- Yang,H, Dou,X, Fang,Y, JiangP,"Self-assembled biomimetic superhydrophobic hierarchical arrays."J. Colloid Interface Sci.,405 51–57 (2013).

8- Xue,CH, Jia,ST, Zhang,J, Ma,JZ,"Large-area fabrication of superhydrophobic surfaces for practical applications: an overview."Sci. Technol. Adv. Mater.,11 (3) 033002-1 (2010).

9- Hui,X, Zhu,Z, Yang,J, Zhu,X. "Study of the corrosion resistance and loading capacity of superhydrophobic meshes fabricated by spraying method."Colloid Surf.A, 377 (1) 70–75 (2011).

10- Chen,X, Yuan,J, Huang,J, Ren,K, Liu,Y, Lu,S, Li, H, "Large-scale fabrication of superhydrophobic polyurethane/nano-Al_2O_3 coatings by suspension flame spraying for anti-corrosion applications."Appl. Surf. Sci.,311864-869 (2014).

11- Celia,E, Darmanin,T, Givenchy,ET, De, Amigoni,S,Guittard,F, "Recent advances in designing superhydrophobic surfaces."J. Colloid Interface Sci., 402 1–18 (2013).

12- Liu,Y, Li,S, Zhang,J, Wang,Y, Han,Z, Ren,L,"Fabrication of biomimetic superhydrophobic surface with controlled adhesion by electrodeposition."Chem. Eng. J.,248 440–447 (2014).

13- Wang,J, Li,D, Liu,Q, Yin,X, Zhang,Y, Jing,X, Zhang,M, "Fabrication of hydrophobic surface with hierarchical structure on Mg alloy and its corrosion resistance."Electrochim.Acta, 55 (22) 6897–6906 (2010).

14- Su,F, Yao,K, Liu,C, Huang,P,"Rapid Fabrication of Corrosion Resistant and Superhydrophobic Cobalt Coating by a One-Step Electrodeposition."ESC Electrochim. J., 160 (11)D593-D599 (2013).

15- Liu, C, Su, F, Liang, J, Huang, P, "Facile fabrication of superhydrophobic cerium coating with micro-nano flower-like structure and excellent corrosion resistance." Surf.Coat.Technol., 258, 580-586 (2014).

16- Chen,A, Chen,Z, Hao,L, Song,Q, Chen,C,"A rapid one-step process for fabrication of superhydrophobic surface by electrodeposition method."Electrochim.Acta, 59168–171 (2012).

17- Chen,Z, Hao,L, Chen,C,"Simultaneous Fabrication of Superhydrophobic Coatings on Cathodic and Anodic Copper Surfaces with Micro / Nano-Structures."ESC Electrochim.Lett.,1 (4) D21–D23 (2012).

18- LiW, KangZ.Fabrication of corrosion resistant superhydrophobic surface with self-cleaning property on magnesium alloy and its mechanical stability.Surf.Coat.Technol.,253 205-213 (2014).

19- Chen,Z, Tian,F, Hu,A, Li,M, "A facile process for preparing superhydrophobic nickel films with stearic acid."Surf.Coat.Technol., 23188–92 (2013).

20- Sun,J, Zhang,F, Song,J,Wang,L, Qu,Q,Lu,Y,Parkin,I,"Electrochemical fabrication of superhydrophobic Zn surfaces."Appl. Surf.Sci., 315346–352 (2014).

21- Chen,Z, Li,F, Hao,L, Chen,A, Kong,Y,"One-step electrodeposition process to fabricate cathodic superhydrophobic surface." Appl. Surf.Sci.,258 (4) 1395–1398 (2011).

22- Liu,T, Yin,Y, Chen,S, Chang,X, Cheng, S, "Superhydrophobic surfaces improve corrosion resistance of copper in seawater."Electrochim.Acta,52 (11) 3709–3713 (2007).

23- Chen,Z, Hao,L, Chen,C, "A fast electrodeposition method for fabrication of lanthanum superhydrophobic surface with hierarchical micro-nanostructures." Colloids Surf.A, 4011–7 (2012).

24- Lluveras,A, Boularand,S, Andreotti,A,"Degradation of azurite in mural paintings: distribution of copper carbonate, chlorides and oxalates by SRFTIR."Appl. Phys.A, 99 (2) 363-375 (2010).

25- Feng,X, J, Jiang,L,"Design and creation of superwetting/antiwetting surfaces."Adv. Mater., 18 (23) 3063–3078 (2006).

26- Cui,Z, Wang,Q, J, Xiao,Y, Su,C, H, Chen,Q,M,"The stability of superhydrophobic surfaces tested by high speed current scouring." Appl. Surf. Sci.,254 (10), 2911–2916 (2008).

27- She,Z, Li,Q, Wang,Z, Tan,C,Zhou,J, Li,L,"Highly anticorrosion, self-

cleaning superhydrophobic Ni–Co surface fabricated on AZ91D magnesium alloy. "Surf. Coat. Technol., 251, 7-14 (2014).

28- [28] YanshengY, LiuT, ChenS, LiuT, ChengS. Structure stability and corrosion inhibition of super-hydrophobic film on aluminum in seawater. Appl. Surf. Sci.12, 255 (5) 2978-2984 (2008).

29- [29] Abbas R, Hefnawy A, El-Dessouky WI, El-Halag A, Sadik WA, El-Demerdash AM. Effect of Durable Superhydrophobic FS/PS Using DCTES on Carbon Steel. J Mater Sci Eng, 7 (1) 408 (2018).

30- [30] El Dessouky WI, Abbas R, Sadik WA, El Demerdash AGM, Hefnawy A. Improved adhesion of superhydrophobic layer on metal surfaces via one step spraying method. Arab. J. Chem. 10 (3) 368-377 (2015).